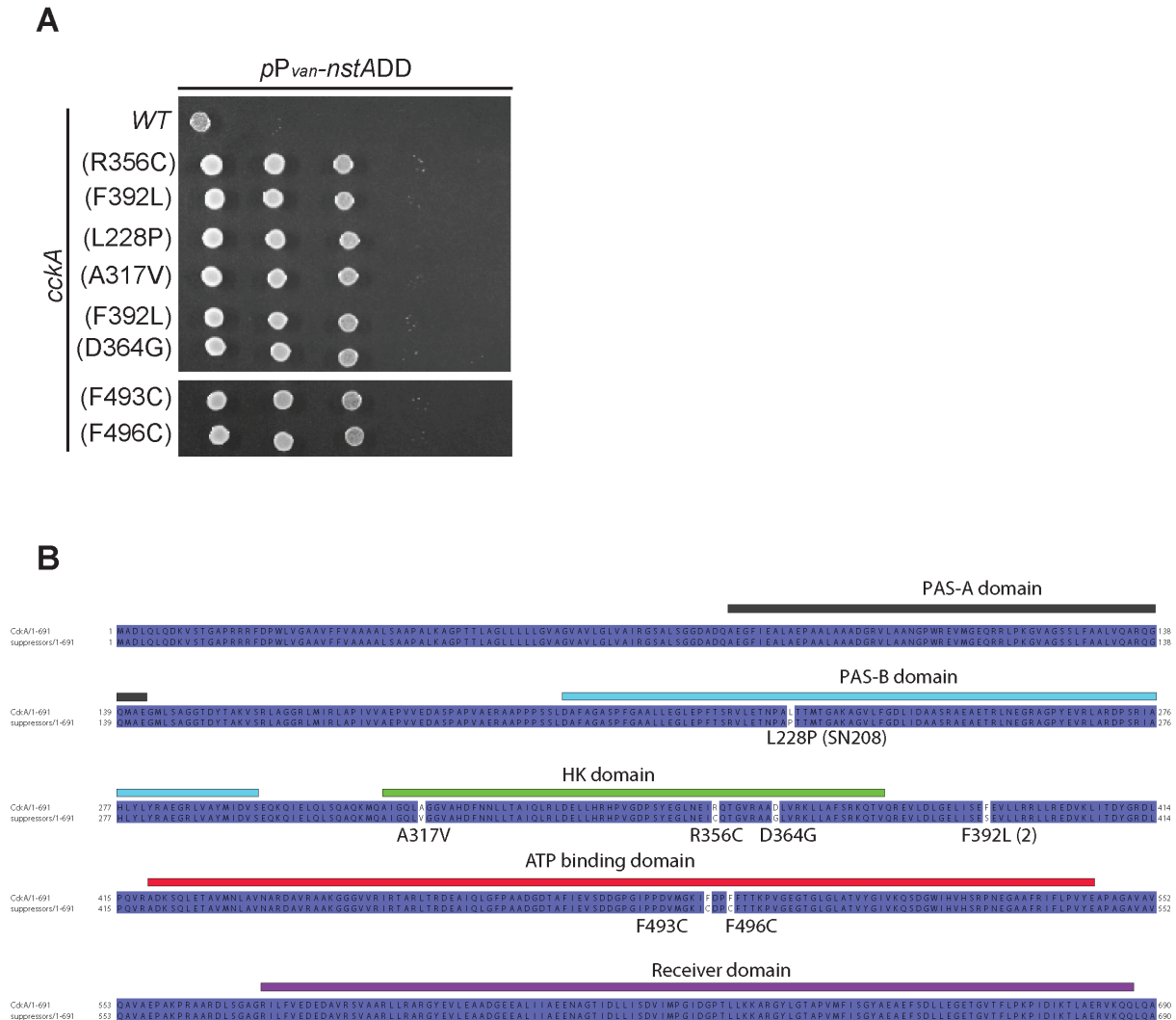
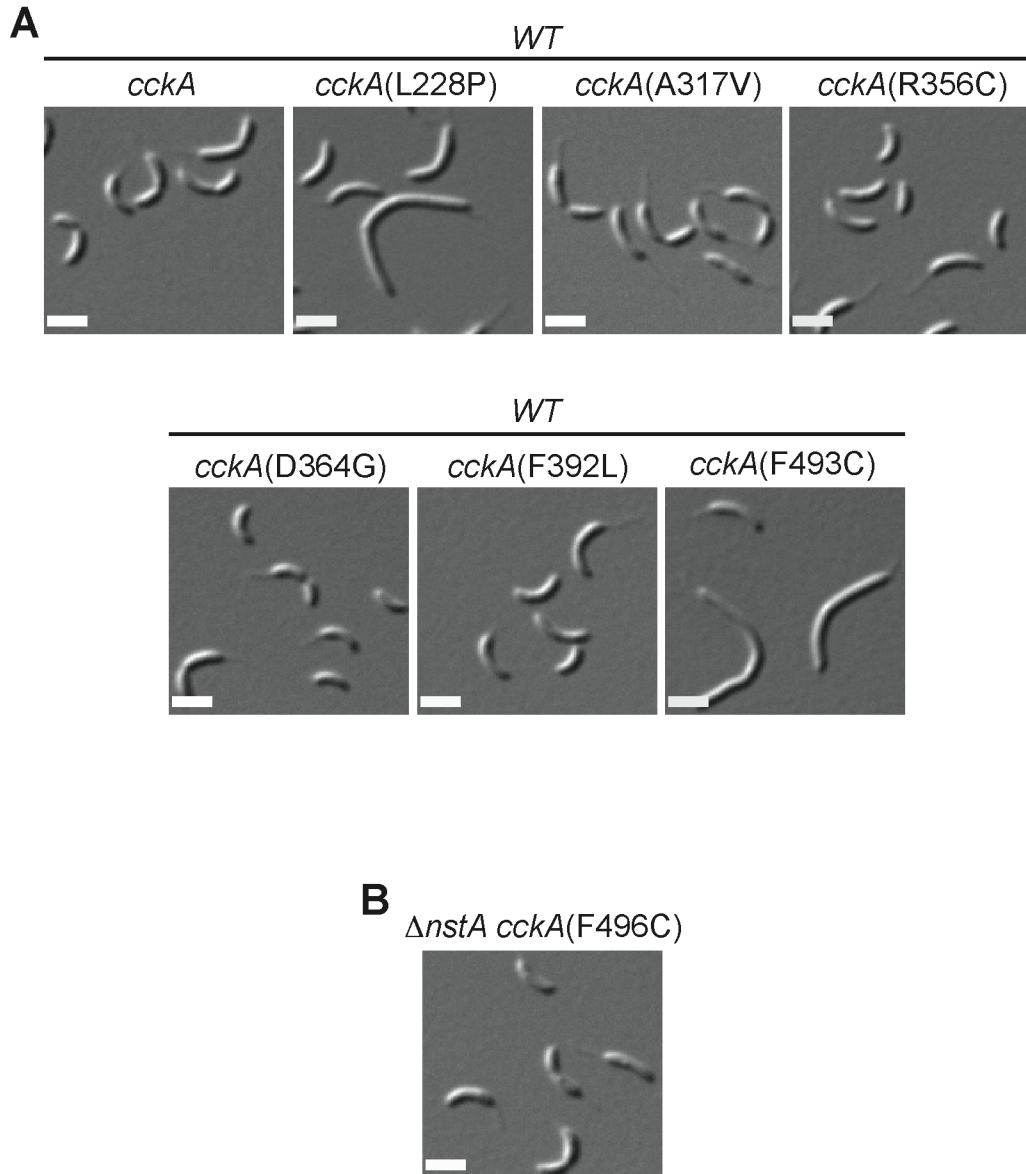


# Sensory domain of the cell cycle kinase CckA regulates the differential DNA binding of the master regulator CtrA in *Caulobacter crescentus*

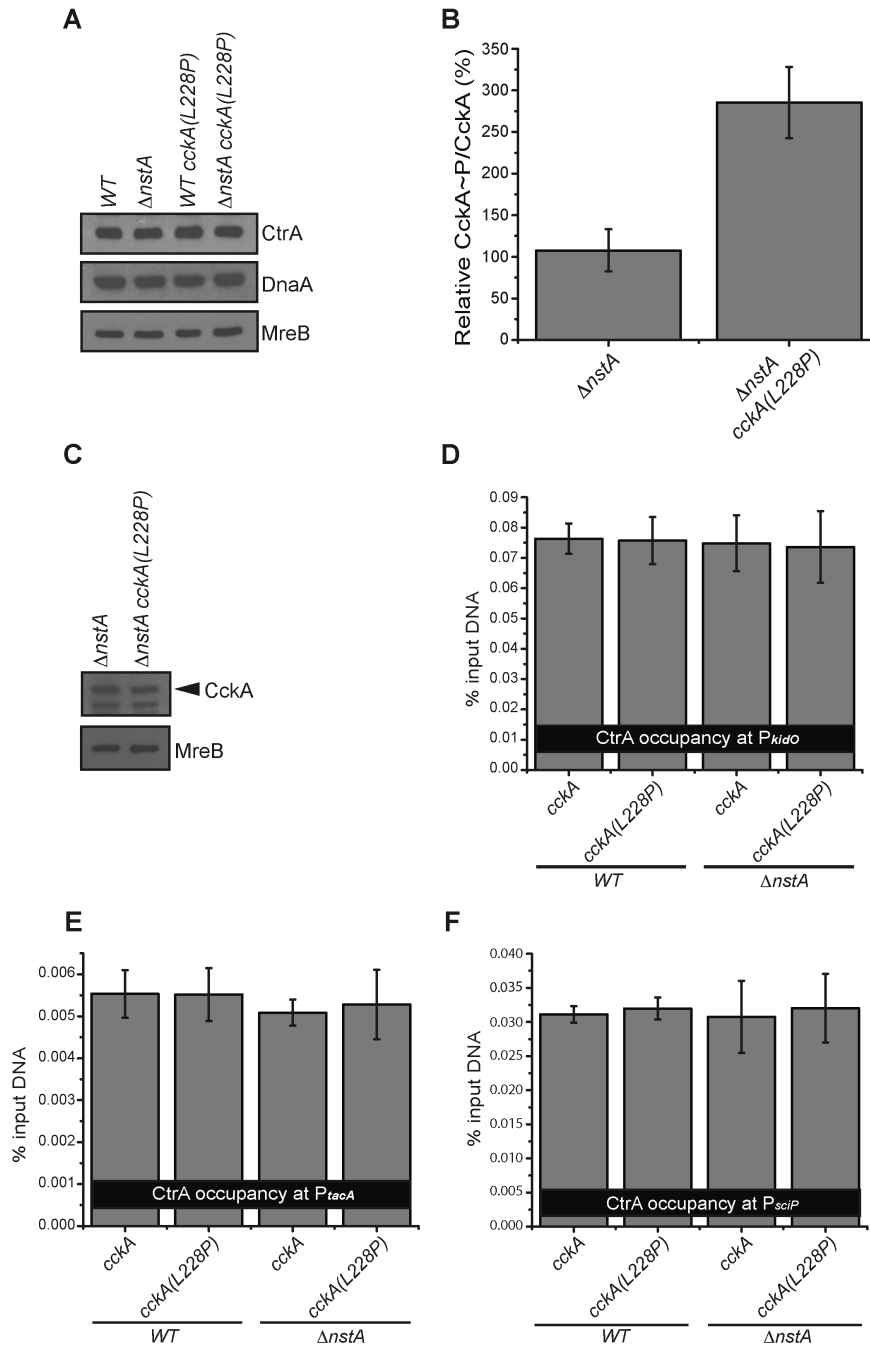
## SUPPLEMENTARY INFORMATION



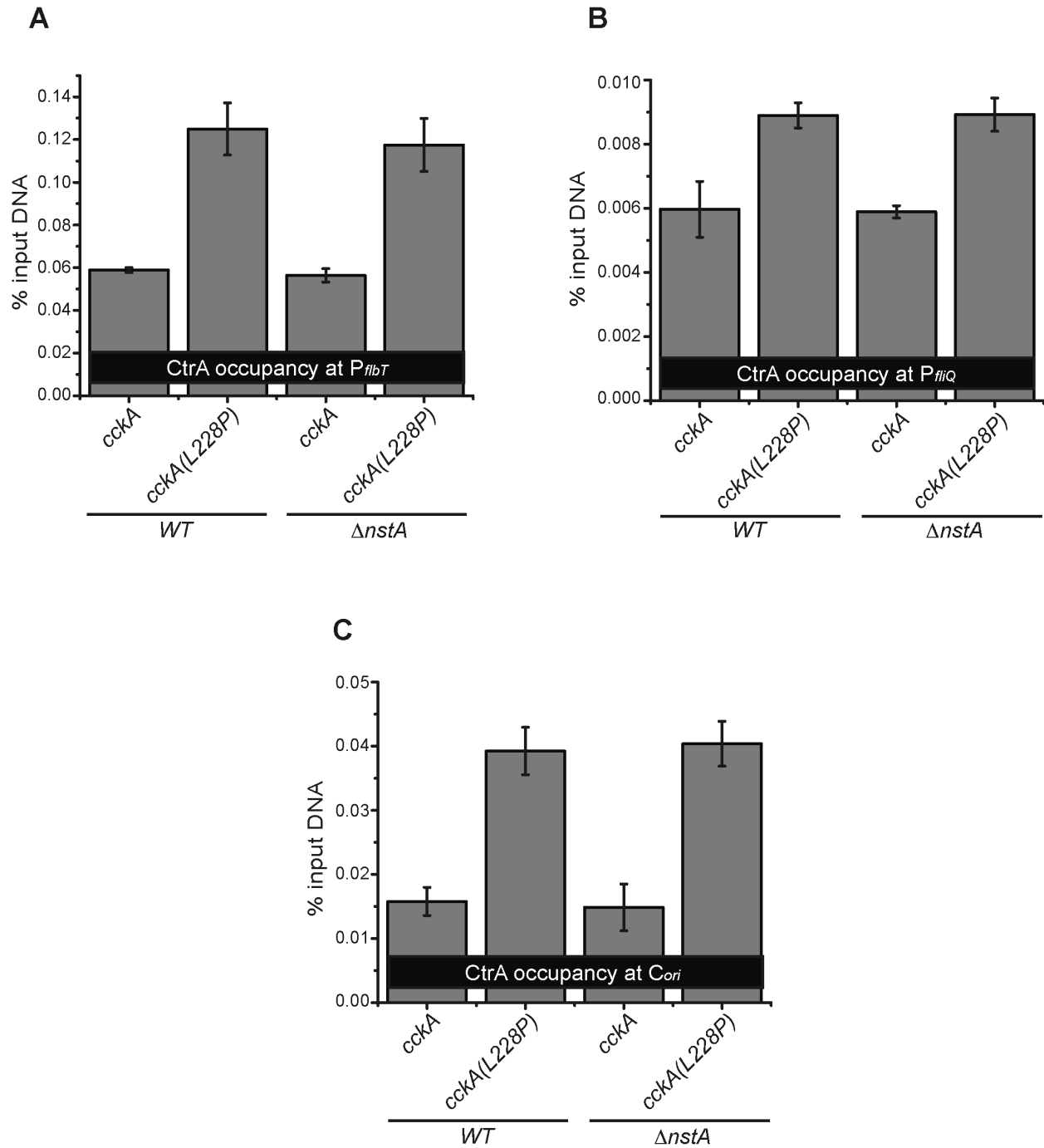
**Supplementary Figure S1.** (A) Growth of *Caulobacter* harboring the *wild-type cckA*, or *NstADD* toxicity suppressor mutants of *cckA*, upon *nstADD* overexpression. The cells were diluted five-fold and spotted on media containing 0.5mM vanillate. The mutant *cckA*(F496C) is in the  $\Delta nstA$  genetic background, rest are in the *WT* background. The only copy of *cckA* on the chromosome is mutated. (B) Schematic denoting the CckA suppressor mutations. The CckA(L228P) mutation resides in the PAS-B domain, whereas the other mutations are harbored either in the histidine kinase domain or the ATP binding domain of CckA.



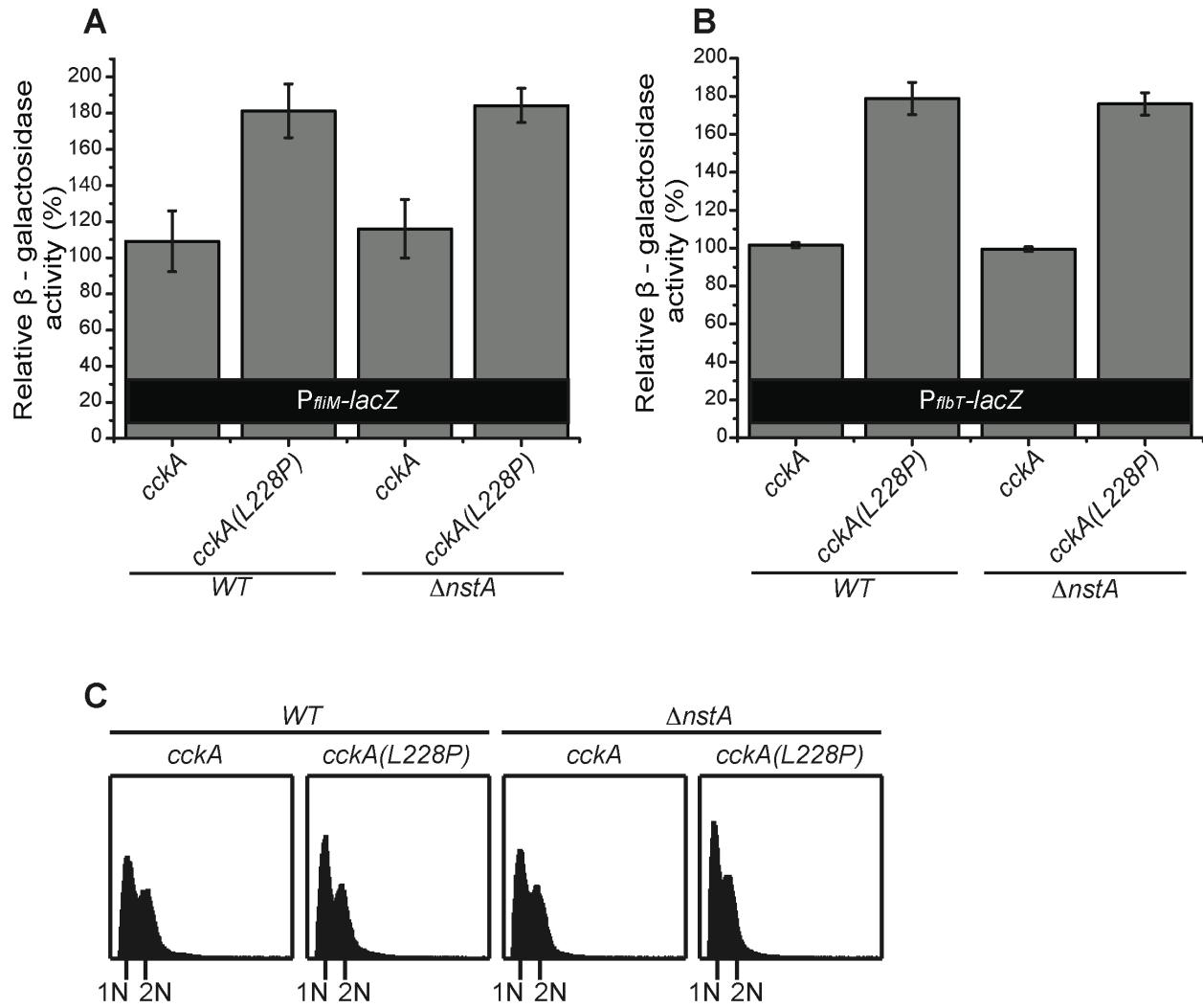
**Supplementary Figure S2.** DIC images of the plasmid-cured suppressor mutants of *cckA* that alleviate the NstADD overexpression toxicity, in (A) wild-type (*WT*) or (B)  $\Delta$ *nstA* backgrounds. In both (A) and (B), the only copy of *cckA* on the chromosome is mutated.



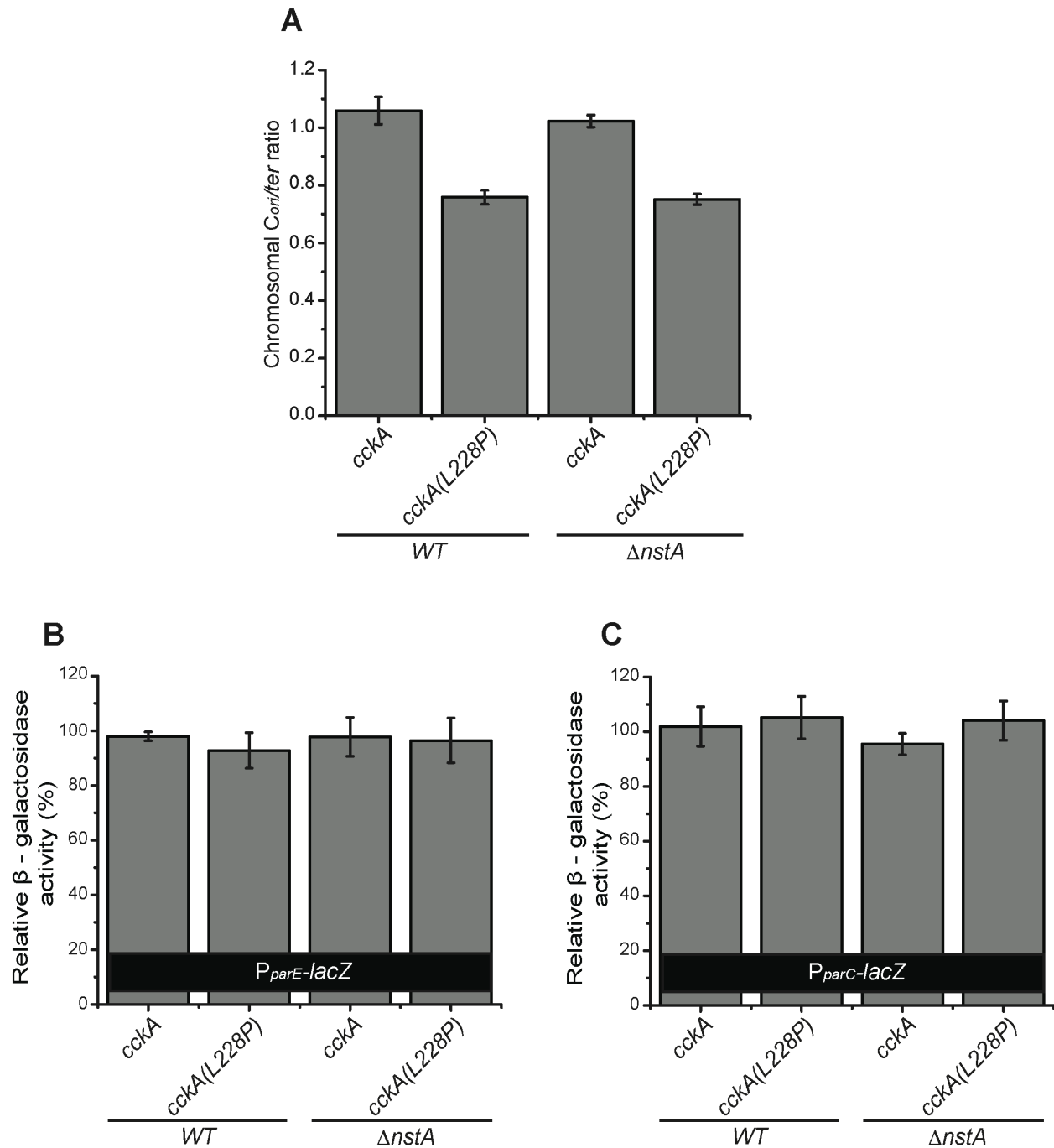
**Supplementary Figure S3.** (A) Immunoblots showing the steady state levels of CtrA and DnaA in *WT*,  $\Delta nstA$ , *WT cckA(L228P)* and  $\Delta nstA cckA(L228P)$  genetic backgrounds. MreB serves as the loading control. (B) *In vivo* phosphorylation experiment depicting the CckA~P/CckA levels in  $\Delta nstA$  and  $\Delta nstA cckA(L228P)$  mutants. (C) Immunoblots showing the total CckA and MreB levels in the cell lysates from  $\Delta nstA$  and  $\Delta nstA cckA(L228P)$  mutants used in (B). The qChIP data indicating the CtrA occupancy at (D) the promoter of *kidO* ( $P_{kidO}$ ), (E) the promoter of *tacA* ( $P_{tacA}$ ), and (F) the promoter of *sciP* ( $P_{sciP}$ ) in *WT*, *WT cckA(L228P)*,  $\Delta nstA$ , and  $\Delta nstA cckA(L228P)$  cells. The data represented in (B), (D), (E) and (F) are the average of three independent experiments,  $\pm$ SE.



**Supplementary Figure S4.** qChIP data indicating the CtrA occupancy at (A) the promoter of *fibT* ( $P_{fibT}$ ), (B) the promoter of *fliQ* ( $P_{fliQ}$ ), and (C) at the chromosomal origin of replication,  $C_{ori}$  in WT, WT *cckA(L228P)*,  $\Delta nstA$ , and  $\Delta nstA$  *cckA(L228P)* cells. The data represented are the average of three independent experiments,  $\pm$ SE.



**Supplementary Figure S5.** Relative  $\beta$ -galactosidase activities of (A)  $P_{fim}$ -lacZ reporter, and (B)  $P_{fibT}$ -lacZ reporter, in WT, WT *cckA(L228P)*,  $\Delta nstA$ , and  $\Delta nstA$  *cckA(L228P)* cells. The values,  $\pm$ SE, in (A) and (B) are the average of three independent experiments. (C) Flow cytometry profiles showing the DNA content in WT, WT *cckA(L228P)*,  $\Delta nstA$ , and  $\Delta nstA$  *cckA(L228P)* cells.



**Supplementary Figure S6.** (A) Relative  $C_{ori/ter}$  ratio obtained from qPCR on chromosomal DNA extracted from *WT*, *WT cckA(L228P)*,  $\Delta nstA$ , and  $\Delta nstA cckA(L228P)$  cells. Values were normalized to a control strain, which corresponds to the *WT* strain grown in PYE medium and treated with rifampicin for three hours. Relative  $\beta$ -galactosidase activities of (B)  $P_{parE-lacZ}$  reporter, and (C)  $P_{parC-lacZ}$  reporter in *WT*, *WT cckA(L228P)*,  $\Delta nstA$ , and  $\Delta nstA cckA(L228P)$  cells. The data represented in (A), (B) and (C) are the average of three independent experiments,  $\pm$ SE.

<b>Strain number</b>	<b>Mutation in CckA</b>	<b>Other mutations</b>
LK128	F392L	None
LK135	D364G	CCNA_01909-(G147A)
LK137	F392L	CCNA_00364-(V208A), CCNA_01161-(G437G)
SN208	L228P	Intergenic SNP between CCNA_01536 and CCNA_01535, Intergenic SNP between CCNA_00614 and CCNA_00615.
LK124	F493C	CCNA_02093-(I457S), CCNA_02487-(G26C), CspC(A63A)
LK98	R356C	None
LK100	F496C	None
LK109	L228P	None
LK122	A317V	CspC(E54D), CCNA_03812-(A110P)

**Supplementary Table S1.** List of the polymorphisms identified from the nine extragenic suppressor strains that alleviated the NstADD overexpression toxicity.

## Supplementary Methods

### Flow cytometry analyses

Flow cytometry analyses were performed as described earlier (26). Cells were incubated at 29°C until mid-log phase, and 1 mL of culture was transferred into 9 mL of ice-cold 70% ethanol and stored overnight at -20°C for fixation. Two milliliters of the fixed cells were washed with 1 mL of staining buffer (10 mM Tris-HCl at pH 7.20, 1 mM EDTA, 50 mM sodium citrate, 0.01% Triton-X-100). The cells were then harvested by centrifugation at 8000 rpm for 5 min, and the pellet was resuspended in 1 mL of staining buffer containing 0.1 mg/mL RNase A (Roche) and incubated for 30 min at room temperature. The cells were pelleted at 8000 rpm for 5 min, and the pellet was resuspended in 1 mL of staining buffer containing 0.5 µM SYTOX green nucleic acid stain (Molecular Probes). The cells were incubated in the dark for 5 min and analyzed using an Accuri C6 flow cytometer (BD Biosciences) equipped with an argon ion laser. Relative chromosome number was directly estimated from the green fluorescence (FL1-A) value of the stained cells and analyzed using BD Accuri C6 software.

### *C<sub>ori</sub>/ter* ratio determination

The *C<sub>ori</sub>/ter* ratios were determined as previously described (32). Cells at the mid-log phase were harvested and chromosomal DNA was extracted using DNAzol reagent and 2 µL of Ready-lyse (250U/µL). The following primer pairs were used for the qPCR reaction: Cori\_fwd (5'-CGCGGAACGACCCACAAACT-3') and Cori\_rev (5'-CAGCCGACCGACCAGAGCA-3') targeting a region close to the origin (*Cori*): Ter\_fwd



(5'-CCGTACGCGACAGGGTCAAATAG-3') and Ter\_rev (5'GACGCGGCGGGCAACAT-3') targeting a region close to the terminus (*ter*). Reactions were run using SYBR Green Supermix (Biorad) in a volume of 20  $\mu$ L, containing 10  $\mu$ L of supermix, 2  $\mu$ L of each pair of primers (concentration 4  $\mu$ M) and 8  $\mu$ L of DNA on a CFX96 Real Time PCR System (Bio-Rad, CA, USA). For quantification of the results, a calibrator-normalized relative analysis was performed using CFX Manager Software for determining the relative abundance of the chromosomal  $C_{ori}$  and *ter* sites in each of the samples. The results were normalized to the  $C_{ori}/ter$  ratio of the wild-type control strain (NA1000) treated with rifampicin for three hours, whose  $C_{ori}/ter$  ratio is almost close to unity.

### Strain construction

The strain **SKR1800** (*WT* + pBVMCS-4-/pMT335- $P_{van}$ -*nstADD*) has been previously described [1].

The various *cckA* point mutant strains namely **SN208** [ $\Delta nstA$  *cckA* (L228P)], **LK98** [*WT cckA*(R356C)], **LK100** [ $\Delta nstA$  *cckA*(F496C)], **LK109** [*WT cckA*(L228P)], **LK122** [*WT cckA*(A317V)], **LK124** [*WT cckA*(F493C)], **LK128** [*WT cckA*(F392L)], **LK135** [*WT cckA*(D364G)] and **LK137** [*WT cckA*(F392L)] were generated by Ultraviolet (UV) radiation based mutagenesis using *WT* or SKR1797 ( $\Delta nstA$ ) [1].

The strains namely **SN227** [ $\Delta nstA$  *cckA* (L228P) + pBVMCS-4- $P_{van}$ -*nstADD*], **SN1140** [*WT cckA*(L228P) + pBVMCS-4- $P_{van}$ -*nstADD*], **SN1141** [*WT cckA*(A317V) + pBVMCS-4- $P_{van}$ -*nstADD*], **SN1142** [*WT cckA*(F493C) + pBVMCS-4- $P_{van}$ -*nstADD*], **SN1144** [*WT cckA*(F392L) + pBVMCS-4- $P_{van}$ -*nstADD*], **SN1145** [*WT cckA*(D364G) +

pBVMCS-4-*P<sub>van-nst</sub>*ADD], **SN1151** [*WT cckA*(R356C) + pBVMCS-4-*P<sub>van-nst</sub>*ADD] and **SN1152** [ $\Delta$ *nstA cckA*(F496C) + pBVMCS-4-*P<sub>van-nst</sub>*ADD] were made by electroporating pSKR126 (pBVMCS-4-*nst*ADD) [1] into SN208 [ $\Delta$ *nstA cckA* (L228P)], LK109 [*WT cckA*(L228P)], LK122 [*WT cckA*(A317V)], LK124 [*WT cckA*(F493C)], LK128 [*WT cckA*(F392L)], LK135 [*WT cckA*(D364G)], LK98 [*WT cckA*(R356C)] and LK100 [ $\Delta$ *nstA cckA*(F496C)] respectively,

The strains **SN377** (*WT*; *xyiX*::*P<sub>xyi</sub>*-*gfp-parB*), **SN379** [ $\Delta$ *nstA cckA*(L228P); *xyiX*::*P<sub>xyi</sub>*-*gfp-parB*] and **SN559** ( $\Delta$ *nstA*; *xyiX*::*P<sub>xyi</sub>*-*gfp-parB*) were made by electroporating pSN190 (pXGFP4C1-*P<sub>xyi</sub>*-*gfp-parB*) into *WT*, SN208 and SKR1797 respectively.

The strains **SN461** [ $\Delta$ *nstA cckA*(L228P) + pJSX-*dnaA*], **SN465** [ $\Delta$ *nstA cckA*(L228P) + pJSX-*dnaA* (R357A)] and **SN467** [ $\Delta$ *nstA cckA*(L228P)+pJS14] were made by electroporating pJSX-*dnaA*, pJSX-*dnaA* (R357A) [2] and pJS14 [3] into SN208 respectively.

The strains **SN505** (*WT*; *xyiX*:: *P<sub>xyi</sub>*-*gfp-parB* + pBVMCS-4) and **SN1153** (*WT*; *xyiX*::*P<sub>xyi</sub>*-*gfp-parB* + pBVMCS-4-*P<sub>van-nst</sub>*ADD) were made by electroporating pBVMCS-4 [4] and pSKR126 into the strain SN377 respectively.

The strains **SN740** (*WT* + pLac290-*P<sub>pilA</sub>*-*lacZ*), **SN742** ( $\Delta$ *nstA* + pLac290-*P<sub>pilA</sub>*-*lacZ*) and **SN744** [ $\Delta$ *nstA cckA*(L228P) + pLac290-*P<sub>pilA</sub>*-*lacZ*] were made by electroporating pJS70 (pLac290-*P<sub>pilA</sub>*-*lacZ*) [5] into *WT*, SKR1797 and SN208 respectively.

The strains **SN741** (*WT* + pLac290-P<sub>*tacA*</sub>-*lacZ*), **SN743** ( $\Delta$ *nstA* + pLac290-P<sub>*tacA*</sub>-*lacZ*) and **SN745** [ $\Delta$ *nstA cckA*(L228P) + pLac290-P<sub>*tacA*</sub>-*lacZ*] were made by electroporating pMV05 (pLac290-P<sub>*tacA*</sub>-*lacZ*) [6] into *WT*, SKR1797 and SN208 respectively.

The strains **SN1361** (*WT* + pLac290-P<sub>*fiiM*</sub>-*lacZ*), **SN1365** ( $\Delta$ *nstA* + pLac290-P<sub>*fiiM*</sub>-*lacZ*) and **SN1369** [ $\Delta$ *nstA cckA*(L228P) + pLac290-P<sub>*fiiM*</sub>-*lacZ*] were made by electroporating pLac290-P<sub>*fiiM*</sub>-*lacZ* into *WT*, SKR1797 and SN208 respectively.

The strains **SN1406** (*WT* + pLac290-P<sub>*flbT*</sub>-*lacZ*), **SN1407** ( $\Delta$ *nstA* + pLac290-P<sub>*flbT*</sub>-*lacZ*) and **SN1408** [ $\Delta$ *nstA cckA*(L228P) + pLac290-P<sub>*flbT*</sub>-*lacZ*] were made by electroporating pLac290-P<sub>*flbT*</sub>-*lacZ* into *WT*, SKR1797 and SN208 respectively.

The *cckA*(L228P) back cross strains **SN739** [*WT*;  $\Delta$ *cckA*(L228P)] **SN769** [ $\Delta$ *nstA*; *cckA*(L228P)] was made by backcrossing the *cckA*(L228P) point mutation in SN208 into *WT* and SKR1797. pSN155 (pNPTS-*cckA* backcross construct) was used to transform SN208 and the transformants were plated on PYE supplemented with Kanamycin. Further  $\phi$ Cr30 lysates of the transformants were made and was used for transducing into *WT* and SKR1797 thereby generating SN 739 and SN769. The backcross strain, SN769, was electroporated with pSKR126, to obtain **SN771** [ $\Delta$ *nstA*; *cckA*(L228P) + pBVMCS-4-P<sub>*van-nstADD*</sub>].

The strains **SN1435** [*WT cckA*(L228P) + pLac290-P<sub>*pilA*</sub>-*lacZ*], **SN1436** [*WT cckA*(L228P) + pLac290-P<sub>*tacA*</sub>-*lacZ*], **SN1437** [*WT cckA*(L228P) + pLac290-P<sub>*fiiM*</sub>-*lacZ*] and **SN1438** [*WT cckA*(L228P) + pLac290-P<sub>*flbT*</sub>-*lacZ*] were made by electroporating pJS70, pMV05, pLac290-P<sub>*fiiM*</sub>-*lacZ* and pLac290-P<sub>*flbT*</sub>-*lacZ* into SN739.

The strains **SN1439** (*WT* + pLac290- $P_{parC}$ -*lacZ*), **SN1441** ( $\Delta nstA$  + pLac290- $P_{parC}$ -*lacZ*), **SN1443** [ $\Delta nstA$  *cckA*(L228P) + pLac290- $P_{parC}$ -*lacZ*] and **SN1445** [*WT* *cckA*(L228P) + pLac290- $P_{parC}$ -*lacZ*], were made by electroporating pLac290- $P_{parC}$ -*lacZ* into *WT*, SKR1797, SN208 and SN739 respectively.

The strains **SN1447** (*WT* + pLac290- $P_{parE}$ -*lacZ*), **SN1449** ( $\Delta nstA$  + pLac290- $P_{parE}$ -*lacZ*), **SN1451** [ $\Delta nstA$  *cckA*(L228P) + pLac290- $P_{parE}$ -*lacZ*] and **SN1453** [*WT* *cckA*(L228P) + pLac290- $P_{parE}$ -*lacZ*], were made by electroporating pLac290- $P_{parE}$ -*lacZ* into *WT*, SKR1797, SN208 and SN739 respectively.

## Plasmid construction

The Plasmid **pBVMCS-4- $P_{van}$ -*nstADD*** is the same as **pSKR126** (pMT335- $P_{van}$ -*nstADD*) described previously [1]. This was made by PCR amplifying *nstADD* (in which the C-terminal Ala-Ala codons were replaced with Asp-Asp [GAU, GAC] codons) and cleaving the fragment with *NdeI* and *EcoRI* and ligating into *NdeI/EcoRI* treated pBVMCS-4 [4].

The plasmid **pSN155** (pNPTS-*cckA*-backcross) construct was made by PCR amplifying a region 750bp upstream of *cckA*. The PCR fragment was digested with *EcoRI/HindIII*. The digested fragment was ligated into pNPTS138 (M.R.K Alley, unpublished) cut with *EcoRI/HindIII*.

Plasmid **pSN190** (pXGFP4-C1- $P_{xyI}$ -*gfp-parB*) was made by PCR amplifying *parB* and cleaving it with *BglII/EcoRI*, wherein the predicted start codon ATG was replaced

with GTG that carried an overlapping *Bg*III recognition site to allow proper placement of *parB* facilitating N-terminal GFP fusion. The alleles were ligated into pXGFP4-C1 vector (M.R.K Alley unpublished) cut with *Bg*III/*Eco*RI.

To make **pSN206** ( $P_{fiiM}$ -*lacZ*, a kind gift from Patrick Viollier) nucleotides 2298862-2299971 of NA1000 genome (CP001340) was amplified and ligated as *Eco*RI/*Hind*III fragment into a medium-copy plasmid pJGZ290 [7] to drive the transcription of the promoterless *lacZ* gene.

Plasmid **pSN209** ( $P_{fibT}$ -*lacZ*, a kind gift from Patrick Viollier) was made by amplifying nucleotides 1633750-1634327 of the NA1000 genome (CP001340) and ligated as *Eco*RI/*Hind*III fragment into the medium-copy plasmid pJGZ290 [7] to drive the transcription of the promoterless *lacZ* gene.

Plasmid **pSN210** (pLac290- $P_{parC}$ -*lacZ*) was made by amplifying nucleotides 1755523-1755922 of the NA1000 genome (CP001340) and ligated as *Eco*RI/*Hind*III fragment into the medium-copy plasmid pJGZ290 [7] to drive the transcription of the promoterless *lacZ* gene.

Plasmid **pSN211** (pLac290- $P_{parE}$ -*lacZ*) was made by amplifying nucleotides 2199977-2200492 of the NA1000 genome (CP001340) and ligated as *Eco*RI/*Hind*III fragment into the medium-copy plasmid pJGZ290 [7] to drive the transcription of the promoterless *lacZ* gene.

Plasmids pJSX-*dnaA*, pJSX-*dnaA* (R357A) and pJS14 were obtained from Justine Collier and are described previously [2, 3].

## References

- [1] S. Narayanan, B. Janakiraman, L. Kumar, S.K. Radhakrishnan, A cell cycle-controlled redox switch regulates the topoisomerase IV activity, *Genes Dev*, 29 (2015) 1175-1187.
- [2] C. Fernandez-Fernandez, D. Gonzalez, J. Collier, Regulation of the activity of the dual-function DnaA protein in *Caulobacter crescentus*, *PLoS One*, 6 (2011) e26028.
- [3] K.C. Quon, G.T. Marczyński, L. Shapiro, Cell cycle control by an essential bacterial two-component signal transduction protein, *Cell*, 84 (1996) 83-93.
- [4] M. Thanbichler, A.A. Iniesta, L. Shapiro, A comprehensive set of plasmids for vanillate- and xylose-inducible gene expression in *Caulobacter crescentus*, *Nucleic Acids Res*, 35 (2007) e137.
- [5] J.M. Skerker, L. Shapiro, Identification and cell cycle control of a novel pilus system in *Caulobacter crescentus*, *Embo J*, 19 (2000) 3223-3234.
- [6] M.V. Marques, S.L. Gomes, J.W. Gober, A gene coding for a putative sigma 54 activator is developmentally regulated in *Caulobacter crescentus*, *J Bacteriol*, 179 (1997) 5502-5510.
- [7] G. Ditta, S. Stanfield, D. Corbin, D.R. Helinski, Broad host range DNA cloning system for gram-negative bacteria: construction of a gene bank of *Rhizobium meliloti*, *Proc Natl Acad Sci U S A*, 77 (1980) 7347-7351.